

Thermal neutron radiation damage on light yield and attenuation length of scintillating fibres

A. Asmone, M. Bertino, C. Bini, G. De Zorzi, G. Diambri Palazzi, G. Di Cosimo, A. Di Domenico, F. Garufi, P. Gauzzi and D. Zanello

Dipartimento di Fisica, Università "La Sapienza", Roma and INFN, Sezione di Roma, Roma, Italy

A. Festinesi

ENEA, Centro Ricerche Energia Casaccia, Roma, Italy

(Received 10 August 1993)

Samples of blue scintillating fibres have been irradiated with thermal neutrons. The light yield and the attenuation length have been measured for a total integrated flux ranging from 3 to 60×10^{13} neutrons cm^{-2} , and for two different fluxes (3.5 and 35×10^9 neutrons $\text{cm}^{-2} \text{s}^{-1}$). The long term damage has been investigated for 2 m long samples with uniform irradiation along the fibre. Sizable deteriorations both in light yield and in attenuation length are found even at our lowest integrated neutron flux.

1. Introduction

Experimental apparatus in high energy physics experiments at the future particle accelerators should operate in a radiation environment much higher than in the past. A particle detection technique which could be very promising, both for calorimetry and tracking purposes, is based on plastic scintillating fibres.

An R&D program on scintillating fibres electromagnetic calorimetry has been carried on in Rome in 1991/92 [1]. We have decided to investigate the effect of neutrons on the fibres performance as: (i) data on scintillating fibres radiation resistance refer mainly to gamma and/or electron effects (like those produced by a ^{60}Co radioactive source); (ii) a large contribution of neutrons to the total radiation is expected at LHC and SSC proton-proton colliders [2]. Our test has been done with a neutron source providing mostly thermal neutrons (98% of the total flux).

Our tests are based on "blue" fibres which have a fast response and whose light is well suited to the standard photocathodes. The scintillating fibres samples have been irradiated in a condition of uniform exposure over the whole fibre length.

The measurement of the average photoelectrons number and the attenuation length has been performed on some commercial types of "blue" scintillating fibres. The effect of a "yellow" optical filter (Kodak Wratten No. 8) has been also investigated.

The "blue" fibres that have been tested are: Bicon

BCF-10, Kuraray SCSF-38, and Kuraray SCSF-81. The scintillating fibres are manufactured by Bicon Corp., Newbury, OH (USA) and Kuraray Co. Ltd., Tokyo (Japan). The samples were provided to us in 1991.

2. Neutron source

The radiation source is the Triga Mark II reactor of the ENEA Centro Ricerche Energia Casaccia near Rome. This reactor operates normally at a power of 1 MW giving a maximum flux of 3×10^{13} neutrons $\text{cm}^{-2} \text{s}^{-1}$.

The energy spectrum of the neutrons from the reactor core entering in the fibre sample volume is given in table 1. The neutron flux is dominated by the thermal component (about 98% of the total neutron flux). Gamma rays are also emitted by the core: the gamma dose is 8×10^{-4} rad/h.

Table 1
Energy spectrum and flux of the neutrons at the fibre position

Neutron energy	Neutron flux [$\text{cm}^{-2} \text{s}^{-1}$]
0 eV-0.26 eV (thermal flux)	3.5×10^{10}
0.26 eV-1.23 keV	4.0×10^8
1.23 keV-0.5 MeV	2.2×10^8
0.5 MeV-2.23 MeV	0.6×10^8
2.23 MeV-10 MeV	0.2×10^8

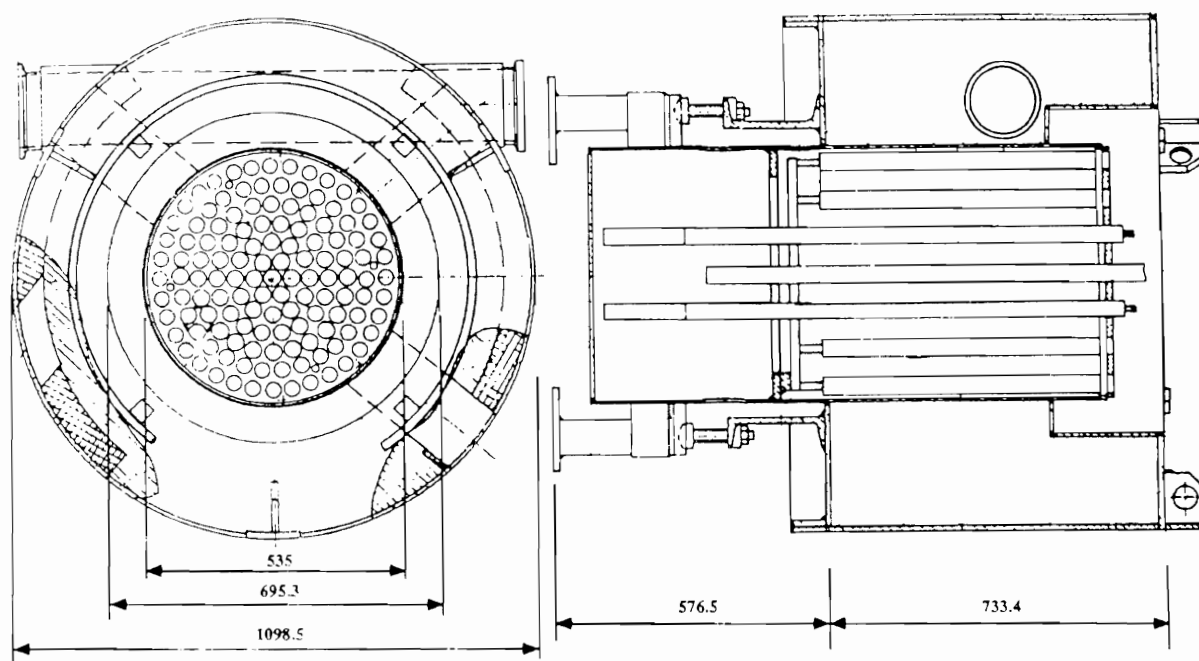


Fig. 1. Schematic view of the reactor core. The fibre sample position during irradiation is also shown.

In order to get a uniform irradiation of the 2 m long scintillating fibres, the sample is bent in a circle and placed on a horizontal plane above the cylindrical core, into the water vessel of the reactor, as shown in fig. 1. The reactor pool water temperature is around 40°C.

The fibre sample is enclosed in a water-proof box of 0.45 m radius of curvature. The box is made of pure aluminium (1 mm thick) in order to avoid long term radioactive contamination. Nevertheless a time interval as long as 3 days after each irradiation is needed before the aluminium box can be opened and the fibre sample analysed.

The addition to the gamma dose due to the gamma rays emitted by the aluminium following neutron captures is negligible.

Hence with the present method only the "long term" radiation damage, i.e. irreversible degradation of the fibre performance, can be measured. "Short term" effects (hence the possible fibre performance recovery) are not investigated.

The fibre sample has been exposed to a flux of 3.5×10^{10} neutrons $\text{cm}^{-2} \text{s}^{-1}$ at the reactor maximum operating power (1 MW). The integrated flux ranges from a minimum value of 3.2×10^{13} neutrons cm^{-2} in 15 minutes exposure time, up to a maximum of 8.9×10^{14} neutrons cm^{-2} in 5 hours.

Moreover a radiation damage dependence on the neutron flux has been investigated turning down the reactor to 100 kW power, corresponding to a 3.5×10^9 neutrons $\text{cm}^{-2} \text{s}^{-1}$ flux.

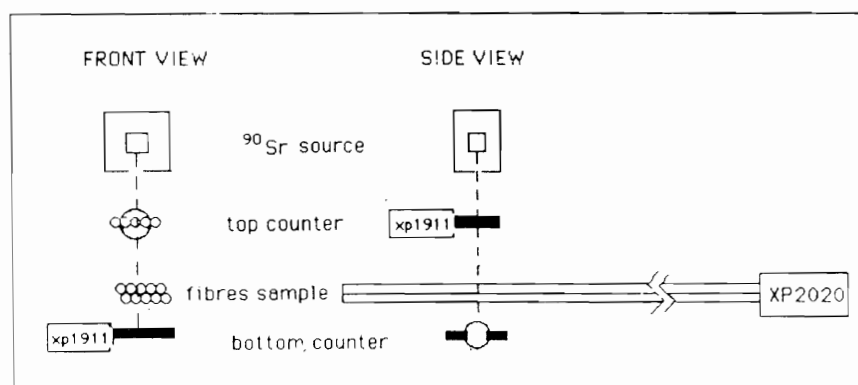


Fig. 2. Schematic view of the fibre test experimental set-up.

3. Experimental set-up

The measurement of the light yield and of the attenuation length of each type of fibre has been done with the experimental set-up schematically shown in fig. 2. A 2 m long bundle of 10 fibres is optically connected to an XP2020 photomultiplier tube (PMT), through Rhodorsil 4 optical grease. The other end of the bundle is simply cut and basically not light reflective. The fibres are staggered in two parallel layers of 5 fibres each, in such a way that the bundle average thickness is 1.57 mm.

A collimated 1 mCi ^{90}Sr radioactive source moves along the fibre bundle on a small tray; the source to PMT distance ranges from 15 to 190 cm.

The PMT signal is gated by the coincidence of two small scintillation counters mounted on the tray. The top counter is located below the source and is made of a layer of five (3 cm long) scintillating fibres parallel to the bundle. The bottom counter is an $8 \times 15 \text{ mm}^2$, 1 cm thick scintillation counter. The fibre bundle under investigation lies in between these two counters.

The PMT output signal is sent to an 11 bits charge integrating ADC LeCroy FERA 4300B gated by a 200 ns signal. The working conditions (i.e. PMT supply high voltage, ADC gate width, counters discriminator threshold) have been kept fixed throughout the measurements.

The PMT gain has been calibrated with a variable light source made of a light emitting diode and two crossed polarising filters. This source allows one to reduce the light reaching the photocathode down to a single photoelectron level. The PMT gain G is evaluated by the anodic charge q collected in the single photoelectron regime; then the number of photoelectrons N is obtained by the simple relation: $q = GeN$.

4. Data analysis and results

Three types of commercial blue scintillating fibres have been tested: BCF-10 by Bicon Co., SCSF-38 and SCSF-81 by Kuraray Co. 2 m long bundles of 10 fibres each have been irradiated as discussed in section 2. The integrated fluxes are given in table 2.

After every irradiation, the light reaching the photocathode as a function of the distance from the PMT has been measured using the experimental set-up described in section 3. For each type of fibre a "zero" measurement has been performed before the irradiation. All measurements have been carried on with and without a yellow filter Kodak Wratten No. 8 interposed between the fibres and the photocathode. The yellow filter cuts away the short wavelength light component ($< 500 \text{ nm}$), hence increases the attenuation length at

Table 2

Light yield and attenuation length relative loss for blue fibres at some integrated fluxes of thermal, epithermal and fast neutrons; the associated gamma rays doses are also quoted. Irradiation is done at a flux of 3.5×10^{10} neutrons $\text{cm}^{-2} \text{ s}^{-1}$. No filter between fibre and PMT photocathode

Fibre	Y_0 loss [%]	λ loss [%]	Neutron integrated flux $\times 10^{13} [\text{cm}^{-2}]$		Gamma rays dose [krad]
			Ther.	(Epi. + Fast)	
BCF10	6	36	3.2	0.06	20
	16	45	6.3	0.13	40
	34	59	12.7	0.26	80
SCSF81	25	48	3.2	0.06	20
	34	53	6.3	0.13	40
SCSF38	19	67	6.3	0.13	40
	30	78	25.3	0.52	160
	61	82	89.0	1.8	560

the expense of a strong reduction (about a factor of 5) of the light collected by the photocathode.

4.1. Light yield and attenuation length dependence on the integrated flux

A typical example of measured light yield Y (average number of photoelectrons/mm) as a function of the distance x from the PMT is shown in fig. 3, for the BCF-10 fibre sample, at four different integrated fluxes F (including the $F = 0$ case). It can be seen that the effect of the radiation damage is: (i) to decrease the light yield at any given distance; and (ii) to make steeper the Y versus x behaviour.

In order to parametrize the F dependence of these two effects, a single-exponential fit has been done on each curve, giving the two parameters Y_0 and λ , Y_0 being the light yield extrapolated at $x = 0$ and λ the attenuation length.

The dependence of Y_0 and $1/\lambda$ on the integrated flux for the three types of fibres measured without the interposition of the yellow filter, is shown in figs. 4 and 5. In table 2 the Y_0 and λ relative losses at the various irradiation conditions are also reported.

4.2. The measurements with the yellow filter

The parameters Y_0 and $1/\lambda$ obtained by measuring the light yield interposing the yellow filter are shown in figs. 6 and 7. Only low integrated flux results are shown because the extremely low level of light for high integrated fluxes does not allow us to quote a reliable result in this case.

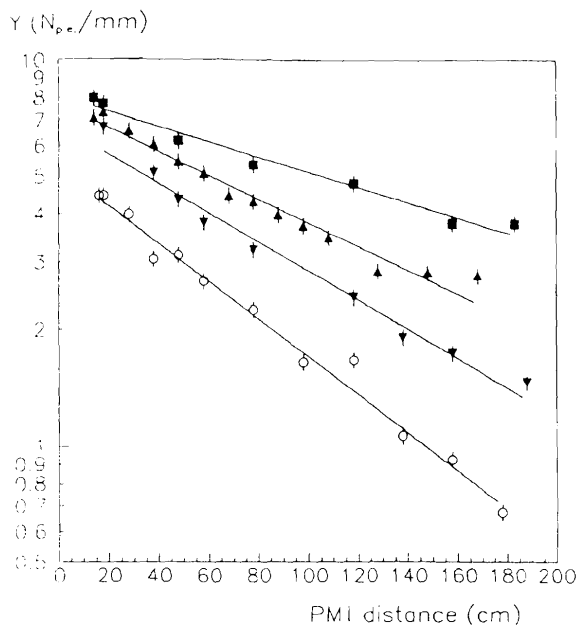


Fig. 3. Average number of photoelectrons per mm as a function of the distance from the PMT for BCF-10 fibres before irradiation (full squares) and after irradiation at three different integrated fluxes: 3.2×10^{13} neutrons cm^{-2} (upward full triangles), 6.3×10^{13} neutrons cm^{-2} (downward full triangles) and 12.7×10^{13} (open circles). Single-exponential fits are superimposed.

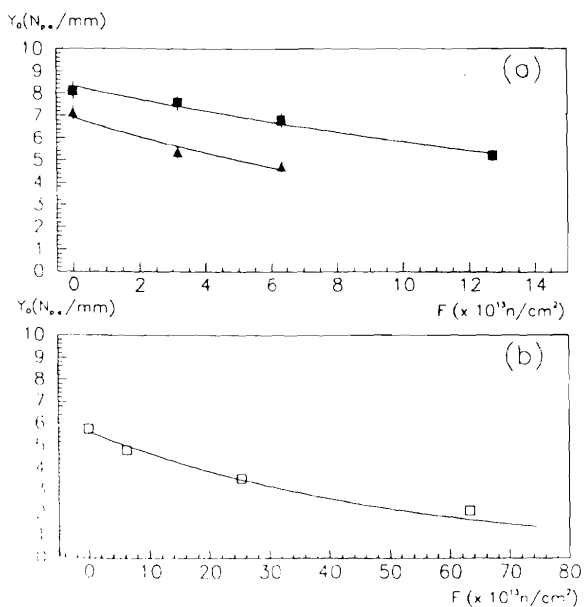


Fig. 4. The light yield extrapolated at $x = 0$ in photoelectrons per mm as a function of the integrated flux F : (a) BCF-10 (full squares), SCSF-81 (full triangles); (b) SCSF-38. Exponential fits according to eq. (1) are shown. For SCSF-38 the highest flux point is not fitted (see text).

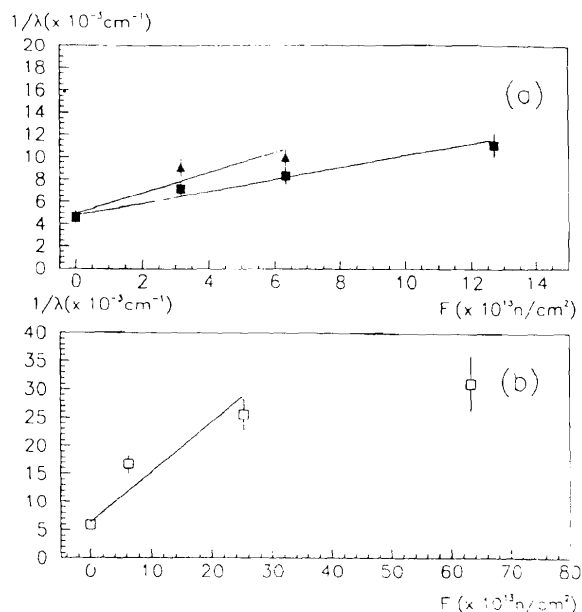


Fig. 5. The inverse attenuation length $1/\lambda$ as a function of the integrated flux F : (a) BCF-10 (full squares), SCSF-81 (full triangles); (b) SCSF-38. Fits according to eq. (2) are shown. For SCSF-38 the highest flux point is not fitted (see text).

By comparing figs. 6 (7) and 4a (5a) it can be argued that the short wavelength light component that is cut away by the yellow filter is more affected by the radiation damage. Therefore the light yield Y_0 and the

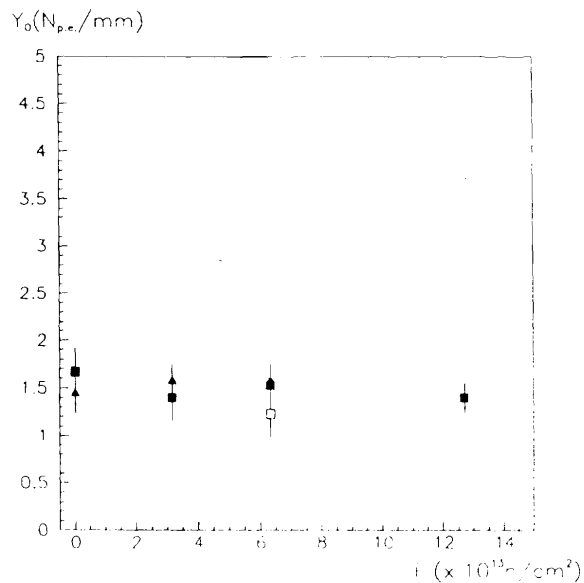


Fig. 6. The same as in fig. 4 from measurements with the yellow filter Kodak Wratten No. 8 interposed between fibres and PMT.

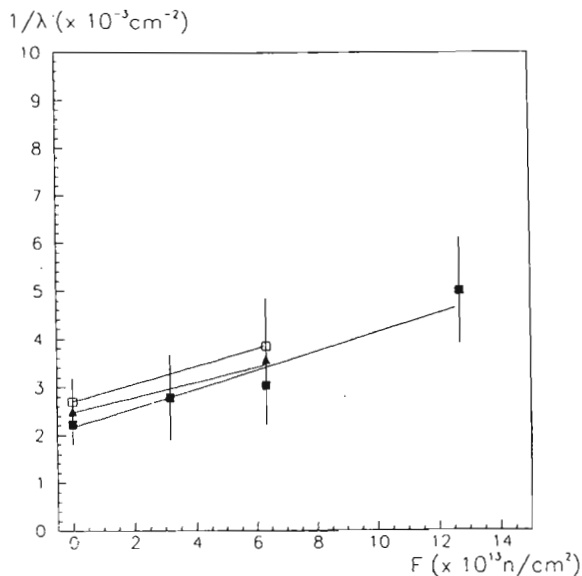


Fig. 7. The same as in fig. 5 from measurements with the yellow filter Kodak Wratten No. 8 interposed between fibres and PMT.

attenuation length λ are both less sensitive to the damage.

4.3. Radiation damage parametrization

A simple parametrization of the dependence of the light yield and of the attenuation length on the integrated flux is given by the expressions [3,4]

$$Y_0(F) = Y_0(0) e^{-F/\gamma}, \quad (1)$$

$$1/\lambda(F) = 1/\lambda(0) + \alpha F, \quad (2)$$

where $Y_0(F)$ and $\lambda(F)$ are the light yield extrapolated at $x=0$ and the attenuation length at an integrated flux F , respectively, and γ and α are two parameters describing the effect of the radiation damage on the light emission and light transmission.

However Acosta et al. have already observed that γ and α are not constant over a large range of integrated fluxes. The same is apparent in our data: in the case of the SCSF-38 fibres, which were exposed to the largest flux range, the last point cannot be included in the fit. Similarly to Acosta et al. we also observe that γ appears to increase and α to decrease with increasing integrated fluxes.

The $Y_0(F)$ experimental data shown in fig. 4 have been fitted with expression (1), and γ values for every type of fibre have been extracted. α values have been obtained by fitting the $1/\lambda(F)$ experimental data shown in figs. 5 and 7 with expression (2).

Table 3

Fitted values of α and γ according to eqs. (1) and (2) for the three types of tested fibres. α_F is the value of α obtained by the "filter" data

	BCF-10	SCSF-81	SCSF-38
$\alpha (\times 10^{-16} \text{ cm})$	0.54	0.92	0.89
$\alpha_F (\times 10^{-16} \text{ cm})$	0.20	0.20	0.20
$\gamma (\times 10^{13} \text{ cm}^{-2})$	28	15	54

In table 3 the obtained values of γ and α are compared for the three fibre types.

In the yellow filter case, as already mentioned in section 4.2, only low integrated flux data could be used, so that γ_F and α_F variation effects, if any, are not seen. In table 3 γ_F is not given since, within our sensitivity, it is essentially infinite.

4.4. Long term damage

As already noted in section 2, the measurement on an irradiated fibres sample has been done about 3-5 days after the irradiation. A further measurement has been performed on the SCSF-38 fibre sample irradiated with 8.9×10^{14} neutrons cm^{-2} 180 days after the exposure. No long term recovery effect has been seen:

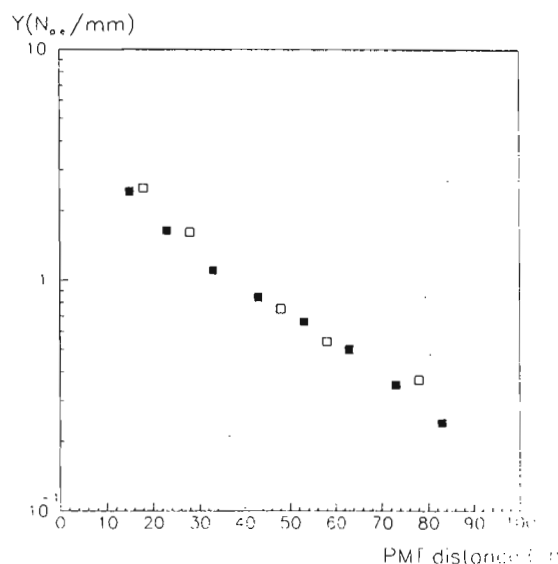


Fig. 8. Comparison between the measurements of the light yield as a function of the distance from the PMT for SCSF-38 fibres irradiated at an integrated flux of 8.9×10^{14} neutrons cm^{-2} , performed after 5 days since the irradiation (full squares) and after 180 days since the irradiation (open squares). The two measurements are in a full agreement so that any recovery effect can be excluded.

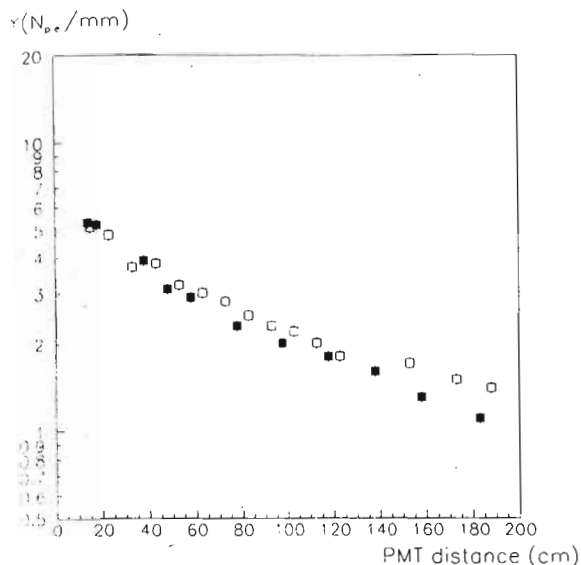


Fig. 9. Comparison between the measurements of the light yield as a function of the distance from the PMT for SCSF-81 fibres irradiated with an integrated flux of 3.2×10^{13} neutrons cm^{-2} at a flux of 3.5×10^9 neutrons $\text{cm}^{-2} \text{s}^{-1}$ (open squares) and 3.5×10^{10} neutrons $\text{cm}^{-2} \text{s}^{-1}$ (full squares). The two measurements are in agreement showing no appreciable flux effect in the explored range of neutron flux.

in fig. 8 a comparison between the two measurements, 5 days and 180 days after the irradiation, is shown.

4.5. Neutron flux effect on damage

For the SCSF-81 fibres the effect of the flux has also been studied. Two samples have been irradiated at the same integrated flux (3.2×10^{13} neutrons cm^{-2}) but at two different fluxes (3.5×10^9 and 3.5×10^{10} neutrons $\text{cm}^{-2} \text{s}^{-1}$). In fig. 9 the measurements on the two samples are compared. The light yield and the attenuation length for the two irradiated samples are quite compatible within the errors. Hence the effect of the flux (in the range 3.5 to 35×10^9 neutrons $\text{cm}^{-2} \text{s}^{-1}$) is negligible.

5. Conclusion

The γ -radiation damage has been investigated for blue scintillating fibres. The irradiation was done by a neutron source with an energy spectrum strongly peaked on the thermal component.

The effects on the performance of the fibres which have a major interest in calorimetry at future very high energy particles accelerators have been measured. Important losses both in light yield and in attenuation length are found when the neutron integrated fluxes exceed 10^{13} neutrons cm^{-2} . On the other hand no effect on the instantaneous neutron flux is observed in the range 3.5 and 35×10^9 neutrons $\text{cm}^{-2} \text{s}^{-1}$. This kind of integrated flux is reached in one year exposure at LHC at $\eta = 1-2$ [2]. However, our two instantaneous fluxes are much higher and are reached at LHC only for $3 < \eta < 5$ [2]. In any event the neutron spectrum calculated in ref. [2] is not similar to ours, containing much harder components.

We wish to point out that, if we refer to the results reported in ref. [4], our γ -ray dose is too small to be responsible for the damage. Likewise, if we refer to the results of ref. [5], our fast neutron flux produces negligible effects on Y_0 and only small effects on λ even at the highest rates. So it appears that the damage reported by us is almost entirely produced by the thermal neutrons.

References

- [1] M. Bertino et al., Nucl. Instr. and Meth. A 315 (1992) 327; A. Asmone et al., Nucl. Instr. and Meth. A 326 (1993) 477.
- [2] G. Stevenson, Large Hadron Collider Workshop, Aachen, 4-9 Oct. 1990, vol. III, p. 566, CERN 90-10, ECFA 90-133; G. Stevenson et al., CERN-TIS-RP 92-07.
- [3] U. Holm and K. Wick, IEEE Trans. Nucl. Sci. NS-36 (1989) 579.
- [4] D. Acosta et al., Nucl. Instr. and Meth. B 62 (1991) 116.
- [5] W.L. Dunn et al., Radiat. Phys. Chem. 41 (1993) 225.